

Exergo-environmental analysis of renewable/waste heat based Organic Rankine Cycle (ORC) using different working fluids

S. Aghahosseini¹, I. Dincer²

Abstract — In this paper, a comprehensive thermodynamic analysis of Organic Rankine Cycle (ORC) using different working fluids driven by renewable/waste low-grade heat sources is conducted, and the performance and environmental characteristics of cycle, especially the potential CO₂ emission, are investigated. The comparative evaluation of cycle using a combined energy and exergy analysis is performed by varying certain system operating parameters such as efficiencies, mass flow rate, cycle irreversibility and heat input at various temperatures and pressures. Moreover the toxicity, flammability, ODP and GWP of different working fluids besides utilizing renewable heat sources are studied as a safety and environmental assessment. The results from this analysis provide valuable insight into selection of the most suitable fluids for power generating applications using low-temperature heat sources.

Keywords — Exergo-environmental analysis, Organic Rankine Cycle, Renewable heat source

1 INTRODUCTION

The Recent major concern of energy industries has been increased utilization of fossil fuels towards global warming, air pollution and ozone depletion. Moreover, waste heat energy being released from process industries and power plants contributes to serious environmental pollution [1]. In this context, utilization of renewable heat based technologies as well as waste heat for electricity production becomes significantly point of interest. Also because the fact that the thermal efficiency of conventional steam power generation becomes uneconomically low when the gaseous steam temperature drops below 371 °C, using water as a working fluid become considerably less efficient and more costly [2].

In recent years, Organic Rankine Cycle (ORC) has become a field of intense research and appears as a promising technology for conversion of low-grade heat into useful work or electricity. The heat source can be of various origins: solar radiation [3], biomass combustion [4], geothermal energy [5] or waste heat from process industries [6, 7]. Some actual applications have been installed for recovering geothermal and waste heat for power generation [8, 9].

Examples are the plants in Altheim, Austria, with a power production of 1MW [10, 11] and in Neustadt-

Glewe, Germany, with a power production of 0.2MW [12]. Unlike in the steam power cycle, where vapour steam is the working ORC cycles employ refrigerants or hydrocarbons. The selection of the working fluid is critical to achieve high thermal efficiencies as well as optimum utilization of the available heat source and also involves various tradeoffs. Moreover, the organic working fluid must be carefully selected based on safety and environmental properties assessment. General criterion such as thermodynamic performance, fluid stability limit, flammability, safety and environmental impact could be used to screen different working fluids. Vijayaraghavan and Goswami [13], Badr et al. [14], Saleh et al. [15], Hettiarachchi et al. [16], Drescher and Brüggemann [17] are some of the researchers who analyzed the characteristics of different working fluids in an ORC application. It can be also seen that the previous studies of ORCs regarded just more about single component organic fluids. However, an important limitation of pure fluids is the constant temperature evaporation which is not suitable for sensible heat sources such as waste heat. The mixtures have variable temperature during the phase change process, which could be used to reduce the mismatch of temperature profiles between heat transfer fluid and the evaporating or condensing working fluid mixtures. So, it can be concluded that the system irreversibilities can be minimized. Wang and Zhao made a theoretical analysis of zeotropic mixtures R245fa/R152a used in low-temperature solar Rankine cycles [18]. Radermacher analyzed the mutual influence of working fluid mixtures properties on the performance of Rankine cycle, and simple counter-flow heat exchangers are suggested in the system for the mixtures [19].

In the present work the energy and exergy analysis of ORC based on potential of different working fluids for

1. S. Aghahosseini is with the Faculty of Engineering and Applied Science, University of Ontario Institute of Technology, 2000 Simcoe Street North, Oshawa, Ontario, Canada, L1H 7K, E-mail: Seyedali.Aghahosseini@uoit.ca

2. I. Dincer is the professor of the Faculty of Engineering and Applied Science, University of Ontario Institute of Technology, 2000 Simcoe Street North, Oshawa, Ontario, Canada, L1H 7K, E-mail: Ibrahim.Dincer@uoit.ca

power production are investigated at various operating conditions. Also, the cycle total irreversibility, required amount of renewable/waste heat for cycle operation and characteristics of selected potential environmentally friendly working fluids are evaluated and compared for a 100kW power system. Besides, due to significant arising interest in using multi-component mixture for ORCs, the exergo-environmental analysis of two different zeotropic mixtures utilized in the low-temperature heat Rankine cycle is provided and compared.

2 METHODOLOGY

The components of an ORC are similar to the conventional Rankine Cycle which consists of a pump, evaporator, expander and condenser. The working fluid is saturated liquid at the exit of the condenser; it is then pumped to the evaporator where it gains heat from the renewable/waste heat source. Hot pressurized working fluid which could be saturated or superheated expands in the expander thereby generate useful work. The layout of an ORC is as shown in Fig. 1. The expander considered here is similar to the scroll expander investigated by Zamfirescu et al. [20] and Quoilin et al. [21].

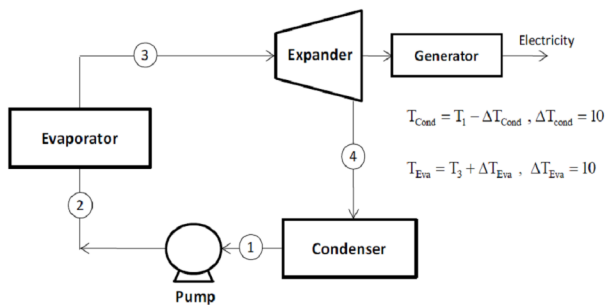


Fig. 1. Schematic of Organic Rankine Cycle.

As it was mentioned earlier, the selection of working fluids and appropriate operation conditions are the most important criteria to system performance. The thermodynamic properties of working fluids will affect the system efficiencies, operating conditions, and environmental impact. Technically, the working fluid can be classified into three categories. Those are dry, isentropic, and wet depending on the slope of the cycle T-s diagram to be positive, infinite, and negative respectively. Also ORC can be classified in two groups according to the level of expander inlet pressure, including supercritical ORCs and sub-critical ORCs; the one which is investigated in the present study.

Figs. 2 and 3 show T-s diagrams of two types of ORC processes with the negative slope of the saturated vapour curve. As is shown in Fig. 2, the working fluid leaves the condenser as saturated liquid, state point 1. Then, it is compressed by the liquid

pump to the sub-critical pressure, state point 2. The working fluid then is heated in the evaporator until it becomes superheated vapour, state point 3. The superheated vapour flow is expanded after to the condensing pressure, state point 4. At the condensing pressure, the working fluid lies in the two phase region. The two phase fluid passes through the condenser where heat is removed until it becomes a saturated liquid, state point 1. The processes in Fig. 3 are similar to those in Fig. 2 with the only difference being that the state point 4 after expansion in the turbine lies in the superheated vapour region.

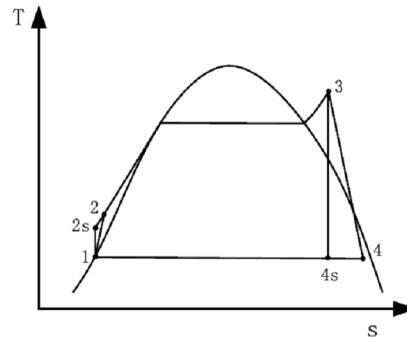


Fig. 2. ORC with negative slope of saturated vapour curve and wet vapour at the expander outlet.

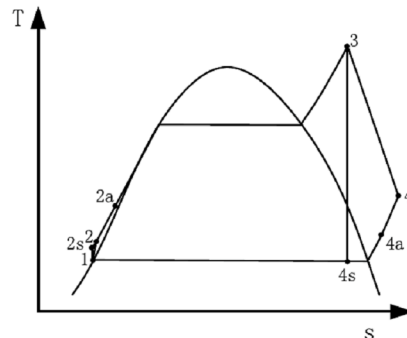


Fig. 3. ORC with negative slope of saturated vapour curve and superheated vapour at the expander inlet.

Figs. 4 and 5 show T-s diagram of the other two types of ORC processes with the positive slope of the saturated vapour curve. The state points 1 and 2 are in the same condition as the ORC system in Figs. 2 and 3. Starting from state 2, the working fluid is heated in the evaporator at constant sub-critical pressure until it becomes saturated, state point 3 in Fig. 3, or it is superheated, state point 3 in Fig. 4. Then, it is expanded to state point 4, which is in the superheated vapour region.

The key point for performance analysis of ORCs which also have been presented by Hung [22], Gurgenci [23], Yamamoto et al. [24], and Somayajiet al. [25] is that the organic working fluid must be operated at saturated vapour condition before expander to reduce the total irreversibility of the system.

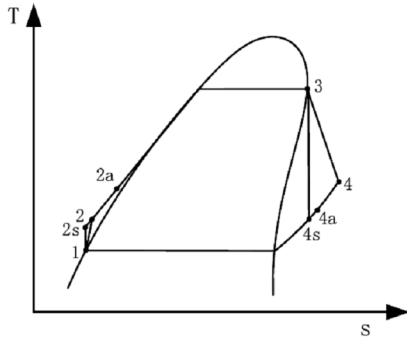


Fig. 4. ORC with non-negative slope of saturated vapour curve and saturated vapour at the turbine inlet.

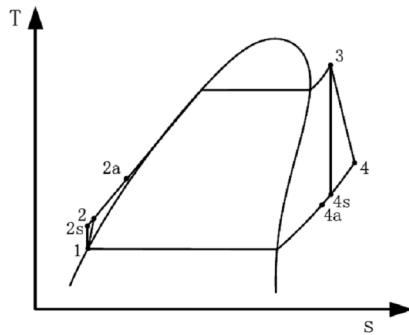


Fig. 5. ORC with non-negative slope of saturated vapour curve and superheated vapour at the turbine inlet.

As it was mentioned earlier, In ORCs application, the selection of working fluid is important since the fluid must not only have thermo physical properties that match the application but also must possess adequate chemical stability at the desired working temperature. Here, working fluids which are chosen they both have almost zero ODP (Ozone Depletion Potential) and lower GWP (Global Warming Potential), which have less environmental impact.

The organic working fluids selected for this investigation are R113, R123, R245fa, R600a, R134a, R407c, and R404a with boiling points ranging from -47 °C to 48 °C. It is found that in the temperature range that a low-temperature heat ORC system works (usually below 200 °C), few pure organic working fluids are isentropic. Most of them are dry or wet. Wet working fluids include R407c, R404a, R134a, and R143a while the dry working fluids include R113, R245fa, R123, and R600a. Table 1 provides physical properties and Table 2 represents safety and environmental data of considered working fluids.

Table 1. Physical properties of the working fluids

Working fluids	Physical Properties		
	T_{bp} (°C)	T_c (°C)	P_c (Mpa)
R113	47.6	214.1	3.44
R123	27.8	183.7	3.66
R245fa	25.13	174.42	3.93
R600a (Isobutane)	-11.7	135	3.64
R134a	-26.1	101	4.06
R407c (R134a, R125, R32)	-43.6	86.8	4.597
R404a (R134a, R125, R143a)	-46.39	72	3.719

T_{bp} : normal boiling point.

T_{crit} : critical temperature.

P_{crit} : critical pressure.

Table 2. Safety and environmental data of the working fluids

Working fluids	Safety Data	Environmental Data		Atmospheric life time (yr)
	ASHRAE safety group	ODP	GWP (100years)	
R113	A1	1	6130	85
R123	B1	0.02	77	1.3
R245fa	A1	0	950	7.6
R600a (Isobutane)	A3	0	8	1
R134a	A1	0	1430	14
R407c (R134a, R125, R32)	A1	0	1800	5
R404a (R134a, R125, R143a)	A1	0	3.26	—

ODP: ozone depletion potential, relative to R11.

GWP: global warming potential, relative to CO₂.

S: Separation occurred in atmosphere

3 SYSTEM MODELLING

For the cycle performance modelling, various operating conditions are analyzed and compared for mentioned working fluids in order to determine the operating condition that presents the best thermal efficiency with minimum irreversibility. This evaluation is performed using a combined first and second law analysis by varying certain system operating parameters at various reference temperatures and pressures. The thermodynamic properties of fluids and system performance are evaluated with a simulation tool Engineering Equation Solver, EES [26]. It is assumed that the system reaches a steady state, and pipe pressure drop and heat losses to the environment in the evaporator, condenser, expander and pump are neglected. Because of the thermodynamic irreversibility occurring in each of the components, such as non-isentropic expansion, non-isentropic compression and heat transfer over a finite temperature difference, the exergy analysis method is employed to evaluate the performance for low grade heat recovery. Consider $P_0=100$ kPa and $T_0=25$ °C to be the ambient pressure and temperature as the specified dead reference state. The isentropic efficiencies of the expander and pump are assumed 85% and 80%, respectively. The condenser temperature was kept constant at 25 °C, while the maximum pressure used for fluids is kept 3000 kPa close working fluid critical pressures. The temperature differential of both evaporator and condenser and the

cycle are assumed constant at 10°C. The energy balance equation of the cycle can be expressed as

$$\sum E_{input} - \sum E_{output} = I \quad (1)$$

Also for the cycle calculation, the exergy of any state point is considered as

$$E_i = m \left[(h_1 - h_0) - T_0 (s_i - s_0) \right] \quad (2)$$

The energy efficiency of the ORC is defined on the basis of the first law of thermodynamics as the ratio of the net power output to the provided external heat.

$$\eta_{energy-cycle} = \frac{(W_{output} - W_{input})}{Q_{input}} \quad (3)$$

In order to reflect the ability to convert energy from low grade waste heat into usable work, cycle exergy efficiency which can evaluate the performance for waste heat recovery is calculated as

$$\Psi_{exergy-cycle} = \frac{(W_{output} - W_{input})}{Q_{input} \times \left(1 - \frac{T_0}{T_{evaporator}}\right)} \quad (4)$$

The irreversibility rate for uniform flow condition in any state of the cycle is expressed as

$$\dot{I} = T_0 \frac{ds}{dt} = T_0 \dot{m} \left[\sum s_{out} - \sum s_{in} + \left(\frac{ds_{system}}{dt} \right) + \sum \frac{q_i}{T_i} \right] \quad (5)$$

where “*i*” represent heat transfer for evaporator or condenser and $\left(\frac{ds_{system}}{dt} \right) = 0$ for assumed steady state condition.

$$\dot{I}_{cycle} = \dot{I}_{pump} + \dot{I}_{evaporator} + \dot{I}_{expander} + \dot{I}_{condenser} \quad (6)$$

$$\eta_{isentropic-expander} = \frac{(h_3 - h_4)}{(h_3 - h_{4s})} \quad (7)$$

$$W_{pump} = \frac{v_1 \times (P_2 - P_1)}{\eta_{isentropic-pump}} \quad (8)$$

4 RESULTS AND DISCUSSION

In this part, the results of modelling and detail calculations of ORC using different pure/zeotropic working fluid in the form of sensitivity analysis of thermo-environment parameters. Figs. 6 and 7 show the variation of the cycle energy efficiency with the expander inlet pressure for pure and zeotropic

working fluids respectively while keeping the expander inlet temperature at saturated condition. This figure demonstrates that the system thermal efficiency increases with the increment of the expander inlet pressure. The results are consistent for all working fluids and reveals that higher inlet expander pressure increases both the net work and the evaporator heat which leads to improved thermal efficiency. However, the percentage of increase of the net work is higher than the percentage of increase of the evaporator heat. Therefore, the ratio of the net work and the evaporator heat increases with the turbine inlet pressure.

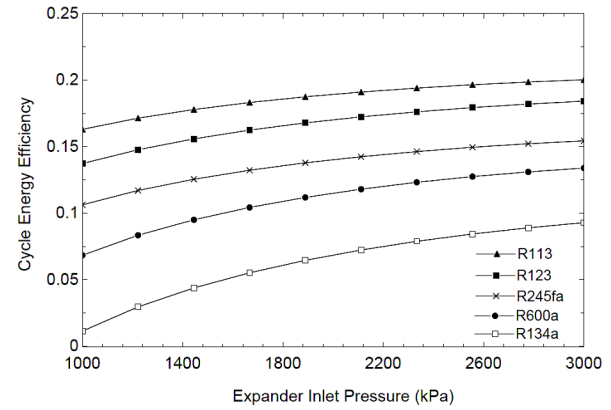


Fig. 6. Variation of ORC energy efficiency with expander inlet pressure for different pure working fluids.

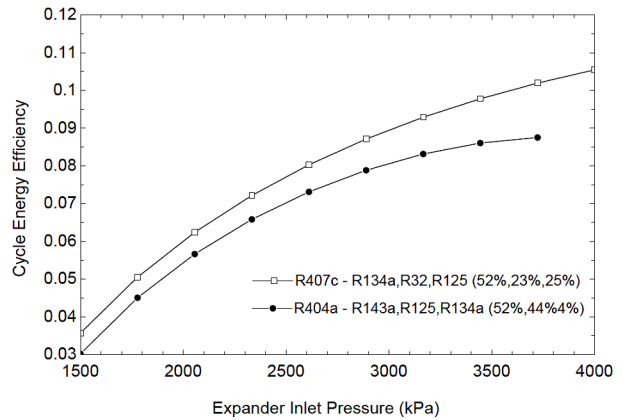


Fig. 7. Variation of ORC energy efficiency with expander inlet pressure for different zeotropic mixture working fluids.

These figures also illustrates that R113 which has the highest boiling point among the selected fluids has the best performance among the other pure organic fluids, while R134a which has the lowest boiling point temperature shows the worst performance. As the result is also the same for zeotropic mixture fluids, therefore, it can be concluded that the higher the boiling point temperature of the working fluid the better the cycle energy efficiency.

Figs. 8 and 9 depict the variation of cycle exergy efficiency with the expander inlet pressure. It is shown that for all mentioned working fluids the exergy efficiency of cycle decrease with the increase in

expander inlet pressure. Due to the fact that decrease in the system exergy efficiency represent an increment in the system irreversibility (higher exergy destruction), this figure provides better understanding of cycle performance and reveals the fact that the higher the boiling point temperature of the working fluid the lower the cycle exergy efficiency.

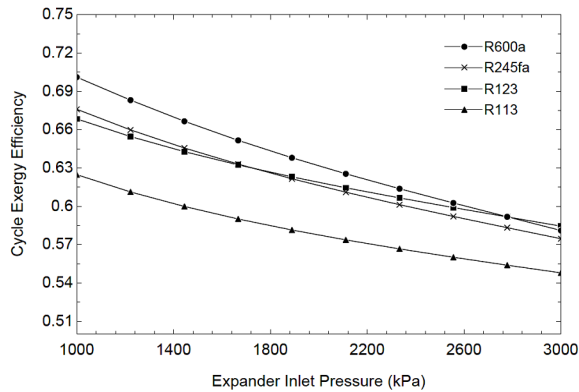


Fig. 8. Variation of cycle exergy efficiency with expander inlet pressure for different pure working fluids.

The cycle exergy efficiency for zeotropic mixtures is highly correlated to temperature of specified expander inlet pressure. The fact is that the result should be considered just for specific range of pressure in different operating conditions.

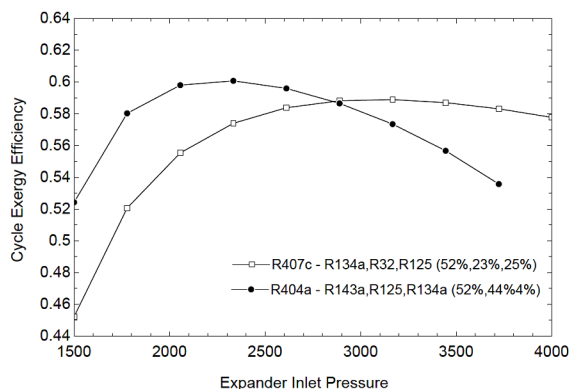


Fig. 9. Variation of cycle exergy efficiency with expander inlet pressure for different zeotropic mixture working fluids.

Figs. 10 and 11 show the effects of the expander inlet pressure on the system irreversibility. In Fig. 10, the system total irreversibility decreases faster for low boiling points zeotropic mixture fluids as the operation pressure at the expander inlet increases and reaches a limit of 3 kW. The lowest irreversibility rate is obtained for R404a. In Fig. 11, the system total irreversibility increases as the pressure at the turbine inlet increases for high boiling point working fluids. For this category, the system irreversibility is lower compared to fluids with low boiling points temperature. In this analysis also the effect of heat source temperature on the system irreversibility could be revealed while keeping the working fluid state along the vapour saturation curve assuming 10 °C

temperature differences between the heat source and expander inlet state.

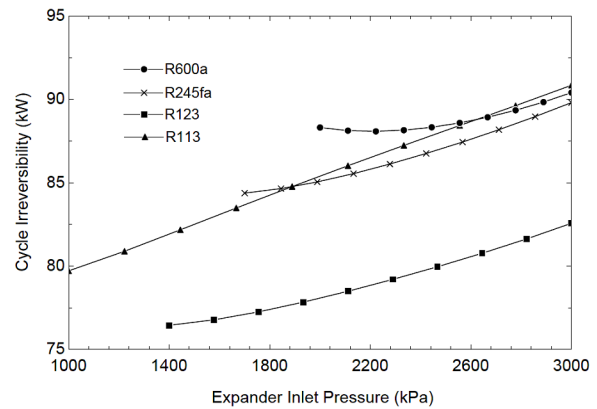


Fig. 10. ORC total irreversibility rate versus expander inlet pressure for working fluids (pure fluids) with high normal boiling points.

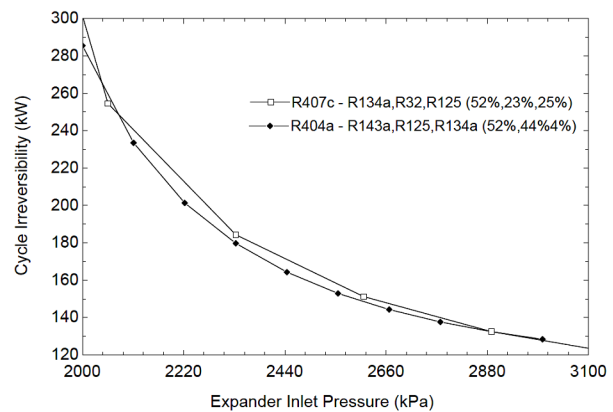


Fig. 11. ORC total irreversibility rate versus expander inlet pressure for working fluids (zeotropic mixture) with low normal boiling points.

The heat transfer rate required in the evaporator to generate the same power output with the expander inlet pressure is evaluated in Figs. 12 and 13. These figures are generated using different working fluids for the different configurations using the same assumptions described above and for an electric power output of 100 kW. It is assumed that the generator convert expander shaft power to electricity without loss. It can be seen that the heat rate needed decreases with increasing expander inlet pressures. This is due to the decrease in the mass flow rate needed and the increase in the net work of the cycle with the increment in expander inlet pressure.

Figs. 14 and 15 show the mass flow rate needed for the cases analyzed in Figs. 12 and 13. It can be seen that the required mass flow rate decreases with the increment of the expander inlet pressure. This is because of the increase in the net work of the cycle with the increment in expander inlet pressure. The results are in line with the results presented in Figs. 6 and 7 since an increment of the net work represents an increase in the cycle energy efficiency.

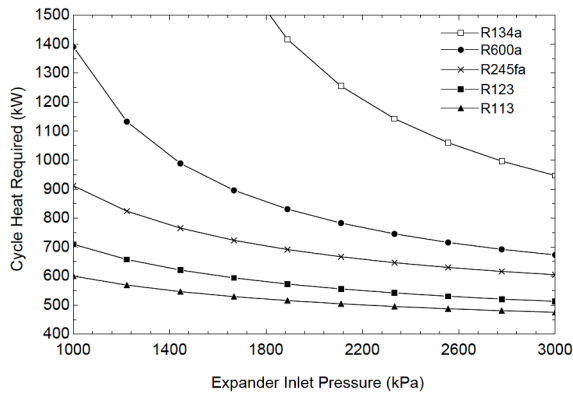


Fig. 12. Variation of cycle heat required with expander inlet pressure for different pure working fluids to produce 100 kW of electric power.

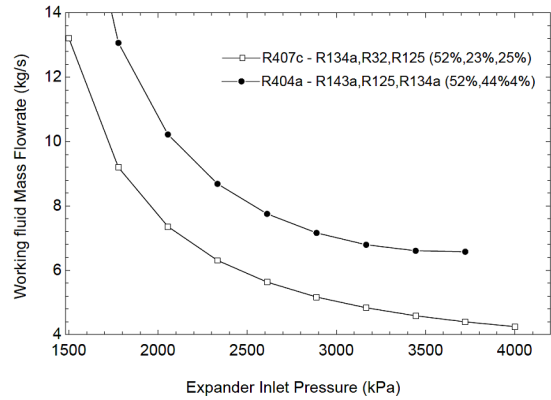


Fig. 15. Variation of cycle working fluid mass flow rate with expander inlet pressure for different zeotropic mixture working fluids in 100 kW electric power production.

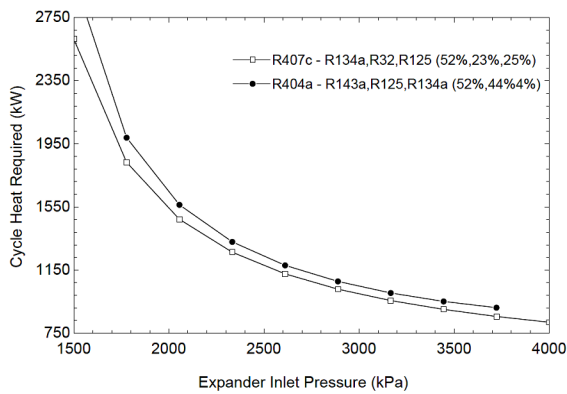


Fig. 13. Variation of cycle heat required with expander inlet pressure for different zeotropic mixture working fluids to produce 100 kW of electric power.

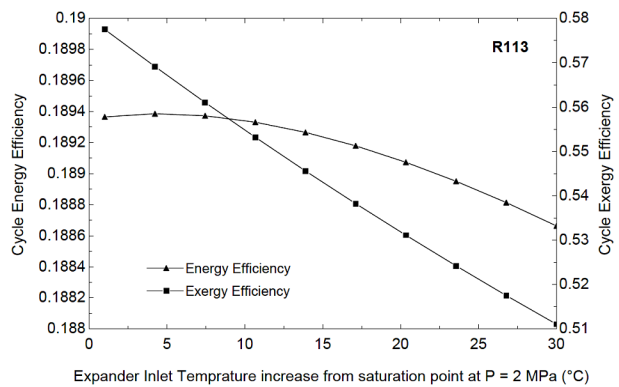


Fig. 16. Variation of cycle energy and exergy efficiency with expander inlet temperature increase from saturation point at P=2 MPa for R113

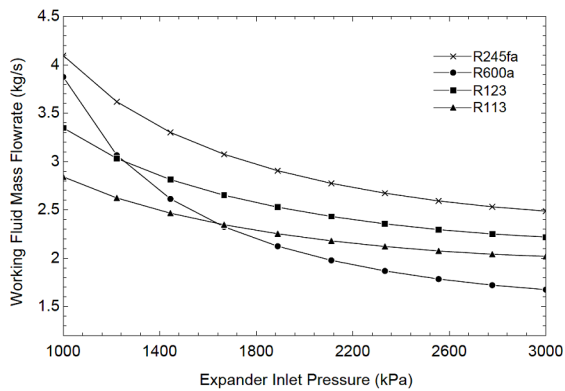


Fig. 14. Variation of cycle working fluid mass flowrate with expander inlet pressure for different pure working fluids in 100 kW electric power production.

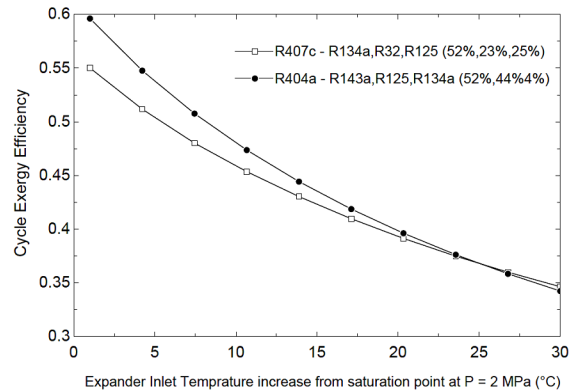


Fig. 17. Variation of cycle energy and exergy efficiency with expander inlet temperature increase from saturation point at P=2 MPa for R407c and R404a

It can be also understood that fluids with lower maximum pressures and higher enthalpy heat of evaporation require low mass flow rate and hence lower heat input. The variation of the cycle energy and exergy efficiency with the expander inlet temperature is analyzed for all working fluids but is depicted in Figs. 16 and 17 just for R113, R407c and R404a because of similar behaviour. It should be also mentioned that evaporation pressure is kept constant at 2 MPa.

These figures reveal the effect of superheating the working fluid on thermal and exergetic efficiency of the cycle. The temperature range is from saturation temperature of each working fluid at P=2 MPa to 30 °C above that point. It is illustrated that the energy efficiency of the cycle slightly decreases for some fluids or remains approximately constant for others and also the exergy efficiency decreases with the increment of the expander inlet temperature. This reflects the fact that organic fluids do not need to be

superheated to increase the cycle thermal efficiency as opposed to water where increasing the inlet turbine temperature increases the thermal efficiency. However, it should be considered that organic fluids are restricted to a small range of applicability depending on their thermodynamic conditions.

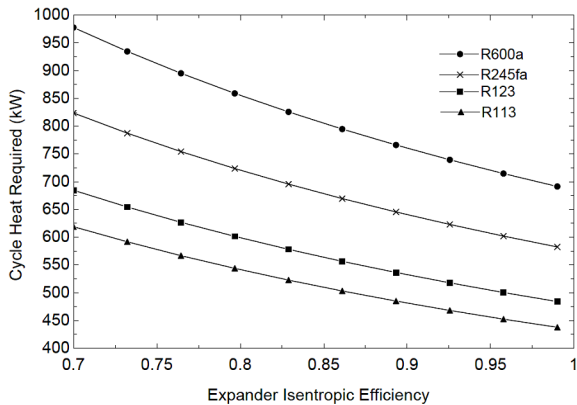


Fig. 18. Variation of cycle heat required with expander isentropic efficiency at inlet pressure 2 MPa for 100 kW electric power production.

Fig. 18 represents the variation of ORC required heat with isentropic efficiency of expander. It is shown that the increases in isentropic efficiency of expander results in significant decrease in amount of external required heat and consequently rise in the cycle efficiencies for specified amount of power production. It can be concluded that choosing different types of expander thoroughly affect cycle performance.

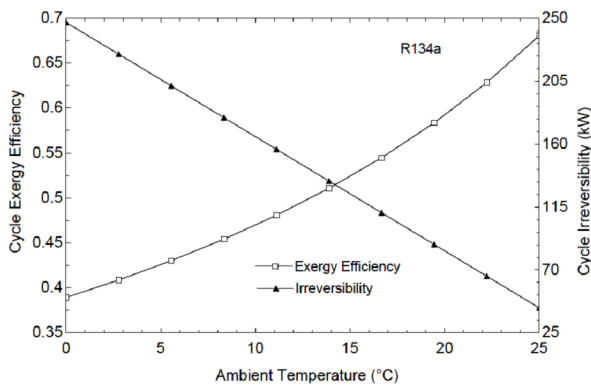


Fig. 19. Exergy efficiency and cycle total irreversibility versus ambient temperature for R134a

Fig. 19 shows the effects of the ambient temperature on the performance of the system. The fluid used for the analysis is the R134a. Technically ambient temperature greatly affects the condenser. As the ambient temperature gets close to the condenser temperature, the condenser irreversibility and consequently the system total irreversibility is reduced. It can be mentioned that by increasing the ambient temperature the exergy efficiency of the cycle increases and in contrast, cycle irreversibility decreases.

It should be considered that growing need to address reduction of greenhouse gas emissions globally would make renewable/waste heat based ORC technology one of the most promising technical options for reducing CO₂ emissions. With renewable/waste heat inlet temperatures as low as 150°C, it is possible to integrate ORC technology into plant designs or assume standalone system for any residential application to recover electric power which can be internally used or can be sold to the power grid. Consequently, it could be assumed that the more reduction in grid power consumption could result in lower CO₂ emissions.

The specific Carbon Dioxide emission (kgCO₂/Kwh) for different fuel combustion systems are depicted in Fig. 20 and compared with renewable/waste heat based ORC.

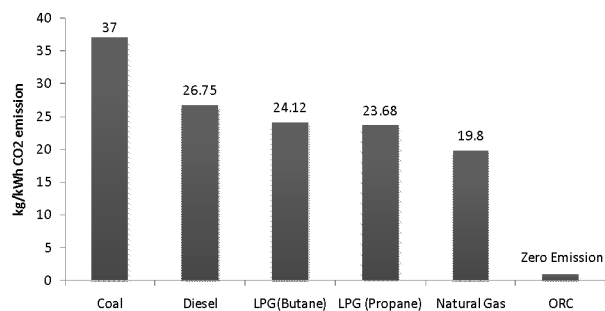


Fig. 20. Kg/kWh CO₂ emission for different fuel combustion system and renewable/waste heat based ORC [27, 28].

It can be revealed that application of ORC using appropriate working fluid for specific operating conditions can substantially contribute to reducing the CO₂ emissions per unit of useful energy produced.

4 CONCLUSIONS

Comprehensive combined energy and exergy analysis of Organic Rankine Cycle for best selection of working fluid is conducted based on utilizing of renewable/waste low-grade heat sources and certain system operating parameters such as efficiencies, mass flow rate and irreversibility at various temperatures and pressures. Also environmental characteristics of selected working fluids such toxicity, flammability, ODP and GWP are studied. The presented comparative evaluation of cycle performance for both pure and zeotropic mixture fluids provides valuable insight into selection of the most suitable fluids for low-temperature applications driven by renewable/waste heat sources based on different application in various operating conditions. It can be concluded that generating electrical power through ORC from renewable heat sources (e.g. solar, geothermal) or recovering low temperature waste heats would significantly reduce CO₂ emissions and offsets grid consumption.

S.Aghahosseini et al: Exergo-environmental analysis of renewable heat based Organic Rankine Cycle (ORC) using different working fluids

REFERENCES

- [1] T.C. Hung, T.Y. Shai, S.K. Wang, A review of organic Rankine cycles (ORCs) for the recovery of low-grade waste heat, *Energy* 22 (7) (1997) 661–667.
- [2] Marciniak TJ, Krazinski JL, Bratis JC, Bushby HM, Buycot EH. Comparison of Rankine-cycle power systems: effects of seven working fluids. Argonne National Laboratory Report ANL/CNSV-TM-87, Illinois; 1981.
- [3] Manolakos D, Kosmadakis G, Kyritsis S, Papadakis G. On site experimental evaluation of a low-temperature solar organic Rankine cycle system for RO desalination. *Solar Energy* 2009; 83:646–56.
- [4] Drescher U, Brüggemann D. Fluid selection for the organic Rankine cycle (ORC) in biomass power and heat plants. *Appl Therm Eng* 2007; 27:223–8.
- [5] Umberto D, Gianni B. Study of possible optimization criteria for geothermal power plants. *Energy Convers Manage* 1997; 38:1681–91.
- [6] Meng Xiangyu, Yang Fusheng, Bao Zewei, Deng Jianqiang, Serge Nyallang N, Zhang Zaoxiao. Theoretical study of a novel solar trigeneration system based on metal hydrides. *Appl Energy* 2010; 87(6):2050–61.
- [7] Liu BT, Chien KH, Wang CC. Effect of working fluids on organic Rankine cycle for waste heat recovery. *Energy* 2004; 29:1207–17.
- [8] Kutscher CF. The status and future of geothermal electric power, NREL/CP-550-28204. Golden, Colorado: National Renewable Energy Laboratory; 2000.
- [9] Bronicki LY, Elovic A, Rettger P. Experience with organic Rankine cycles in heat recovery power plants. Proceedings of the 58th American Power Conference, Chicago, IL. Chicago: Illinois Institute of Technology; 1996, p. 1086–9 [Part 2 (of 2)].
- [10] Gaia M. The Altheim Rankine cycle turbogenerator, 1MWel organic Rankine cycle power plant powered by low temperature geothermal water. In: Geothermische Vereinigung, Geeste, editor *Geothermische Energie*, vol. 36/37(3/4); 2002.
- [11] Kohler S, Saadat A. Möglichkeiten und Perspektiven der geothermischen Stromerzeugung. In: Huenges E, Saadat A, Kohler S, Rockel W, Hurter S, Seibt A, Naumann D, Zimmer M, Erzinger J, Wiersberg Th, Legarth B, Wolff H, editors. *Geothermische Technologieentwicklung: geologische und energietechnische Ansatzpunkte*, Geo-Forschungs-Zentrum Potsdam, Scientific Technical Report STR00/ 23, 2000, p. 7–28 (in German).
- [12] Bromann E, Eckert F, Mollmann G. Technisches Konzept des Kraftwerkes Neustadt-Glewe. In: Geothermische Vereinigung und GeoForschungsZentrum Potsdam, editors. *Start in eine neue Energiezukunft. Tagungsband 1. Fachkongress Geothermischer Strom 12–13 November 2003*, Neustadt-Glewe, ISBN 3-932570-49-9, Geeste 2003.
- [13] S. Vijayaraghavan, D.Y. Goswami, Organic working fluids for a combined power and cooling cycle, *ASME Journal of Energy Resources Technology* 127 (2005) 125–130.
- [14] O. Badr, S.D. Probert, P.W. O'Callaghan, Selecting a working fluid for a Rankine cycle engine, *Applied Energy* 21 (1985) 1–42.
- [15] B. Saleh, G. Koglbauer, M. Wendland, J. Fischer, Working fluids for low temperature organic Rankine cycles, *Energy* 32 (2007) 1210–1221.
- [16] H.D.M. Hettiarachchi, M. Golubovic, W.M. Worek, Yasuyuki Ikegami, Optimum design criteria for an organic Rankine cycle using low-temperature geothermal heat sources, *Energy* 32 (2007) 1698–1706.
- [17] U. Drescher, D. Brüggemann, Fluid selection for the organic Rankine cycle (ORC) in biomass power and heat plants, *Applied Thermal Engineering* 27 (2007) 223–228.
- [18] Wang XD, Zhao L. Analysis of zeotropic mixtures used in low-temperature solar Rankine cycles for power generation. *Solar Energy* 2009; 83:605–13.
- [19] Radermacher R. Thermodynamic and heat transfer implications of working fluid mixtures in Rankine cycles. *Int J Heat Fluid Flow* 1989; 10:90–102.
- [20] C. Zamfirescu, I Dincer. Thermodynamic analysis of a novel ammonia-water trilateral Rankine cycle. *Thermochimica Acta* 477 (2008) 7-15.
- [21] S. Quoilin, M. Orosz, V. Lemort, Modeling and experimental investigation of an organic rankine cycle using scroll expander for small solar applications, in: Proc. Eurosun Conf., Lisbon, Portugal, 7–10 October, 2008.
- [22] T.C. Hung, Waste heat recovery of organic Rankine cycle using dry fluids, *Energy Conversion & Management* 42 (2001) 539–553.
- [23] H. Gurgenci, Performance of power plants with organic Rankine cycles under part-load and off-design conditions, *Solar Energy* 36 (1) (1986) 45–52.
- [24] T. Yamamoto, T. Furuhashi, N. Arai, K. Mori, Design and testing of the organic Rankine cycle, *Energy* 26 (3) (2001) 239–251.
- [25] C. Somayaji, P. Mago, L.M. Chamra, Second law analysis and optimization of organic Rankine cycles, in: ASME Power Conference, Paper No. PWR2006-88061, Atlanta, GA, May 2–4, 2006.
- [26] S.A. Klein, *Engineering Equation Solver (EES)*, Academic Professional Version, 2007.
- [27] CO2 Emissions from Fuel Combustion - IEA Online Database via OECD Library, 2010.
- [28] Carbon Dioxide Emissions from the generation of Electric Power in the United States, DOE, July 2000.